Toxicon 106 (2015) 14–19

Contents lists available at ScienceDirect

Toxicon

journal homepage: www.elsevier.com/locate/toxicon

Functional importance of the Gly cluster in transmembrane helix 2 of the *Bordetella pertussis* CyaA-hemolysin: Implications for toxin oligomerization and pore formation

Sirikran Juntapremjit [a, 1], Niramon Thamwiriyasati [b, 1], Chattip Kurehong [a], Panchika Prangkio [c], Lalida Shank [c], Busaba Powthongchin [d, **], Chanan Angsuthanasombat [a, e, *]

[a] Bacterial Protein Toxin Research Cluster, Institute of Molecular Biosciences, Mahidol University, Nakhon Pathom 73170, Thailand
[b] Department of Medical Technology, Faculty of Allied Health Sciences, Burapha University, Chonburi 20131, Thailand
[c] Department of Chemistry, Faculty of Science, Chiang Mai University, Chiang Mai 50200, Thailand
[d] Department of Biopharmacy, Faculty of Pharmacy, Silpakorn University, Nakhon Pathom 73000, Thailand
[e] Laboratory of Molecular Biophysics and Structural Biochemistry, Biophysics Institute for Research and Development (BIRD), Bangkok 10160, Thailand

ARTICLE INFO

Article history:
Received 9 June 2015
Received in revised form
7 August 2015
Accepted 7 September 2015
Available online 10 September 2015

Keywords:
Adenylate cyclase-hemolysin
GXXGXXXG motif
Helix–helix association
Hemolytic activity
Trimeric pore model

ABSTRACT

Adenylate cyclase-hemolysin (CyaA) is a major virulence factor of *Bordetella pertussis* causing whooping cough in humans. We previously showed that two transmembrane helices (α2 and α3) in the hemolysin domain (CyaA-Hly) are crucially involved in hemolytic activity. Here, PCR-based substitutions were employed to investigate a potential involvement in hemolysis of a series of four Gly residues (Gly^{530}, Gly^{533}, Gly^{537} and Gly^{544}) which map onto one face of a helical wheel plot of pore-lining helix 2. All CyaA-Hly mutant toxins were over-expressed in *Escherichia coli* as 126-kDa soluble proteins at levels comparable to the wild-type toxin. A drastic reduction in hemolytic activity against sheep erythrocytes was observed for three CyaA-Hly mutants, *i.e.* G530A, G533A and G537A, but not G544A, suggesting a functional importance of the Gly^{530}_Gly^{533}_Gly^{537} cluster. A homology-based structure of the α2-loop-α3 hairpin revealed that this crucial Gly cluster arranged as a GXXGXXXG motif is conceivably involved in helix–helix association. Furthermore, a plausible pore model comprising three α2-loop-α3 hairpins implicated that Gly^{530}XXGly^{533}XXXGly^{537} could function as an important framework for toxin oligomerization. Altogether, our present data signify for the first time that the Gly^{530}_Gly^{533}_Gly^{537} cluster in transmembrane helix 2 serves as a crucial constituent of the CyaA-Hly trimeric pore structure.

1. Introduction

Bordetella pertussis, the causative agent of human whooping cough, secretes a variety of potential virulence factors including the 177-kDa adenylate cyclase-hemolysin toxin (known as CyaA) that is indispensable for colonization of this pathogen in the respiratory tract (Melvin et al., 2014). The N-terminal adenylate cyclase (AC) domain complementary to the C-terminal hemolysin (Hly) domain has made CyaA unique from its relative RTX (Repeat-in-ToXin) cytolysins (Linhartova et al., 2010). Nonetheless, the AC domain is not required for hemolytic activity of the Hly domain (Sakamoto et al., 1992; Powthongchin and Angsuthanasombat, 2008). In view of the RTX cytolysins, the CyaA-Hly domain comprises four functional regions (*see* Fig. 1A): a hydrophobic (HP) region containing a number of putative transmembrane helices responsible for pore formation (Bellalou et al., 1990; Powthongchin and Angsuthanasombat, 2009); an acylation region encompassing the conserved Lys^{983} side-chain necessary for toxin activation by CyaC acyltransferase (Hackett et al., 1994); a Ca^{2+}-binding region containing Gly–Asp nonapeptide repeats (X-U-X-Gly-Gly-X-Gly-X-

Abbreviations: CyaA, adenylate cyclase-hemolysin toxin; CyaA-Hly, CyaA-hemolysin domain; PFT, pore-forming toxin; RTX, Repeats-in-ToXin; TM, transmembrane.

* Corresponding author.
** Corresponding author.
E-mail addresses: powthongchin_b@su.ac.th (B. Powthongchin), chanan.ang@mahidol.ac.th (C. Angsuthanasombat).
[1] Authors with equal contributions.

http://dx.doi.org/10.1016/j.toxicon.2015.09.006
0041-0101/

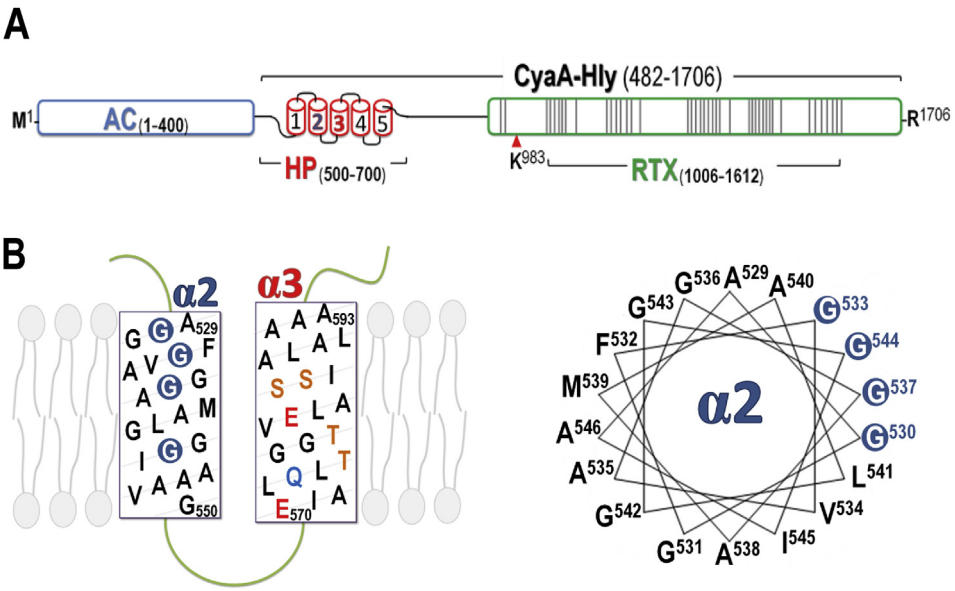

Fig. 1. (A) Schematic diagram of CyaA showing AC (adenylate cyclase) and Hly (hemolysin) domains. Five putative helices in the HP (hydrophobic) region (residues 500–700) are represented by red cylinders. The palmitoylation site is indicated by Lys^{983}, while the Ca^{2+}-binding region (residues 1006–1612) is denoted by multiple lines, with each line corresponding to single nonapeptide repeats (Gly-Gly-X-Gly-X-Asp-X-Leu-X). (B) Schematic representation of two pore-lining helices ($\alpha2_{529-550}$ and $\alpha3_{570-593}$) proposed as a transmembrane hairpin (left panel). The blue shaded circle of white letters in α2 represent the four Gly residues (Gly^{530}, Gly^{533}, Gly^{537} and Gly^{544}) that map onto one face of a helical wheel plot (right panel) in which amino acids are plotted every 100° consecutively around the helix axis. (For interpretation of the references to color in this figure legend, the reader is referred to the web version of this article.)

Asp, X for any amino acid and U for large hydrophobic residues) which fold into a β-roll structure involved in toxin binding to target cells (Guermonprez et al., 2001); and a C-terminal region serving as a signal for toxin secretion (Chenal et al., 2010). Additionally, Ca^{2+} ions were found to be essential for structural stability of the CyaA toxin by incorporating into the Gly–Asp repeat region (Pojanapotha et al., 2011; Karst et al., 2014). Although the molecular mechanistic view of how the CyaA toxin functions has increased substantially over the last two decades (Hackett et al., 1994; Guermonprez et al., 2001; Chenal et al., 2010; Linhartova et al., 2010; Pojanapotha et al., 2011; Karst et al., 2014; Kurehong et al., 2015), the actual underlying mechanism of its toxicity process remains to be investigated.

The secreted CyaA toxin has been shown to bind specifically to the $\alpha_M\beta_2$-integrin receptor (also known as CD11b/CD18) on certain target cells such as human macrophages (Guermonprez et al., 2001). Upon such specific binding, the CyaA-Hly domain would mediate translocation of the catalytic AC domain into the cytosol of target cells to cause a drastic increase in the amount of intracellular cAMP, leading to apoptotic cell death (Cheung et al., 2008; Karst et al., 2010). Besides the AC cytotoxic action on human macrophages, the 177-kDa full-length CyaA toxin, as well as its 126-kDa isolated Hly domain, also exerts hemolytic activity against sheep erythrocytes lacking the CD11b/CD18 receptor (Sakamoto et al., 1992; Powthongchin and Angsuthanasombat, 2008), suggesting a different toxin-induced invasive pathway. Since there is no three-dimensional (3D) structure of RTX cytolysins, the N-terminal HP region of the CyaA-Hly domain has been prefigured to adopt five putative transmembrane helices, *i.e.*, $\alpha1_{(500-522)}$, $\alpha2_{(529-550)}$, $\alpha3_{(570-593)}$, $\alpha4_{(602-627)}$ and $\alpha5_{(678-698)}$, using various algorithms of membrane topology predictions (Powthongchin and Angsuthanasombat, 2009). Further studies *via* single-Pro substitutions as a means of perturbing each individual confined helical structure suggested that the putative α2-loop-α3 hairpin is part of the CyaA-induced pore in the target cell membrane (Powthongchin and Angsuthanasombat, 2009). We have also revealed a functional importance of Glu^{570} which is highly conserved throughout the RTX cytolysin family and located in the tentative pore-lining helix 3 of CyaA-Hly (Kurehong et al., 2011). However, more structural details of membrane-pore formation by the CyaA-Hly domain remain to be explored.

Transmembrane (TM) helix–helix interactions have been proposed to take place through recognition of certain potential motifs ranging from GXXXG and Leu zippers to polar side-chains and salt bridges (Li et al., 2012; Mueller et al., 2014; Walther and Ulrich, 2014). Particularly, the GXXXG motif, with a high occurrence in TM helices, has long been shown to be important in helix–helix interactions prior to molecular assembly (Russ and Engelman, 2000; Senes et al., 2000; Melnyk et al., 2004; Senes et al., 2004). Of particular interest, three of the nine Gly residues (*i.e.* the Gly^{530}_Gly^{533}_Gly^{537} cluster) within the entirely hydrophobic helix 2 of the CyaA-Hly domain can be assigned as a GXXGXXXG motif. In the present study, four Gly residues (Gly^{530}, Gly^{533}, Gly^{537} and Gly^{544}) which are found lining the same side on a helical wheel projection (*see* Fig. 1B, right panel) were therefore initially selected for assessment of their possible involvement in CyaA-Hly activity *via* single-Ala substitutions. Our overall results revealed for the first time that the Gly^{530}_Gly^{533}_Gly^{537} cluster plays a crucial role in hemolysis CyaA-Hly against sheep erythrocytes, conceivably implicated in driving and stabilizing the helix–helix association for toxin oligomerization and pore formation within the target membrane.

2. Materials and methods

2.1. Construction of mutant plasmids

The pCyaAC-PF recombinant plasmid encoding both the 126-kDa CyaA-Hly toxin fragment and the 21-kDa CyaC acyltransferase which is required for toxin activation (Powthongchin and Angsuthanasombat, 2008), was used as a template for single-Ala substitutions. All mutant plasmids were generated by PCR-based

directed mutagenesis using a pair of mutagenic primers (*see* Supplementary Table 1) and Phusion® High-Fidelity DNA polymerase (Finnzymes, Finland), following the procedure of the QuickChange Mutagenesis Kit (Stratagene). PCR products were digested with *Dpn*I to remove the parental DNA template and then transformed into *Escherichia coli* strain JM109. The mutant clones with the required mutation were first identified by restriction endonuclease digestion and subsequently verified by DNA sequencing.

2.2. Expression of mutant toxins

Verified mutant plasmids were retransformed into *E. coli* strain BL21(DE3)pLysS. Each clone harboring the wild-type or its mutated plasmids was grown at 30 °C in Luria-Bertani medium supplemented with ampicillin (100 μg/mL) and chloramphenicol (34 μg/mL). When OD_{600} of the culture reached 0.5–0.6, protein expression was induced with 0.1 mM isopropyl-β-D-thiogalactopyranoside (IPTG) and further incubation for 6 h. After harvesting cells (6000×*g*, 4 °C, 10 min), the pellet was resuspended in 50 mM Tris–HCl (pH 7.4) containing 5 mM $CaCl_2$ and 1.0 mM phenylmethylsulfonylfluoride and subsequently disrupted in a French Pressure Cell (10,000 psi). After centrifugation (12,000×*g*, 4 °C, 20 min), the lysate supernatant was analyzed by SDS–PAGE and its protein concentration was determined by Bradford-based protein microassay using bovine serum albumin as a standard.

2.3. Toxin verification via Western blotting

Toxin samples separated on SDS–PAGE were transferred to a nitrocellulose membrane blocked with 5% skim milk-PBS (120 mM NaCl, 16 mM Na_2HPO_4, 4 mM NaH_2PO_4, pH 7.4) and probed with rabbit anti-RTX antiserum (1:40,000 dilution) as described previously (Kurehong et al., 2015). Immune-complexes were detected with alkaline phosphatase (AP)-conjugated goat anti-rabbit IgG antibodies (Pierce; 1:20,000 dilution) and visualized by incubation with BCIP/NBT (5-bromo-4-chloro-3-indolyl phosphate/nitroblue tetrazolium).

2.4. In vitro hemolytic activity assays

Hemolysis assays were performed against sheep erythrocytes as previously described (Powthongchin and Angsuthanasombat, 2008). 200 μL of whole cell lysate (~1 mg total proteins) containing ~10 μg toxin (estimated by visual comparison of the toxin band intensity with the standard markers in a Coomassie blue-stained gel using a densitometer) were mixed with 800 μL of sheep erythrocyte suspension (5×10^8 cells) in Tris-buffer saline (150 mM NaCl, 2 mM $CaCl_2$, 20 mM Tris–HCl, pH 7.4), and then incubated at 37 °C for 5 h. The released hemoglobin in the supernatant was measured by spectrophotometer at OD_{540}. Cell lysate harboring the pET-17b vector was used as a negative control while 100% hemolysis was obtained by lysing the erythrocytes with 0.1% Triton-X 100. Percent hemolysis of each toxin sample was calculated by [(OD_{540} sample − OD_{540} negative control)/(OD_{540} of 100% hemolysis − OD_{540} negative control)] × 100. All toxin samples were tested in triplicate for at least three independent experiments. The statistical significance of the data between samples was analyzed using Student's *t*-test.

2.5. Homology-based modeling and oligomeric docking

Atom coordinates of α2-loop-α3 hairpin (residues 529–593) were extracted from the 3D model of CyaA-HP comprising α1–α5 which was previously constructed using the best-fit template structure of bovine rhodopsin (1gzm.pdb) (Kurehong et al., 2011). Individual replicas of the extracted hairpin structure were docked to assemble an oligomeric pore complex *via* ZDOCK server (Pierce et al., 2014) prior to energy-minimized *via* GROMACS server (Van Der Spoel et al., 2005). The most promising modeled complex was selected according to energy-based scoring (*i.e.* statistical potential, electrostatics and shape complementarity at protein/protein interfaces) and subsequently analyzed using VMD software (Humphrey et al., 1996).

3. Results and discussion

3.1. Common features of single-Ala substituted CyaA-Hly mutants

As was previously proposed that the putative transmembrane hairpin (*i.e.* α2-loop-α3, *see* Fig. 1B, left panel) which plays a crucial role in hemolytic activity of the CyaA-Hly fragment could conceivably be the pore-lining constituent in which α3 facing the pore lumen is responsible for ion conduction while α2 interacting with the lipid membrane could be involved in toxin oligomerization (Powthongchin and Angsuthanasombat, 2009; Kurehong et al., 2011). Interestingly, when α2 which is entirely hydrophobic throughout a 22-residue segment (A^{529}GGFGVAGGAMALGGGIAAAVG^{550}) was displayed using a helical wheel projection, a series of four Gly residues (Gly^{530}, Gly^{533}, Gly^{537} and Gly^{544}) were located onto one face of the plot (Fig. 1B, right panel). Herein, site-directed mutagenesis was then performed to evaluate a possible contribution of these four individual Gly residues on CyaA-Hly hemolytic activity.

All four Ala-substituted CyaA-Hly mutants (G530A, G533A, G537A and G544A) were successfully generated and efficiently expressed in *E. coli* upon IPTG induction together with the 21-kDa accessory protein, *i.e.* CyaC acyltransferase (*see* Fig. 2A). Additionally, all the 126-kDa mutant proteins were highly produced as

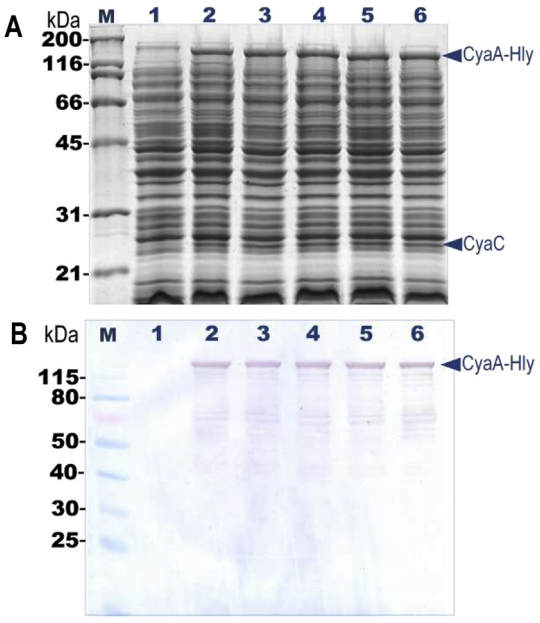

Fig. 2. (A) SDS–PAGE (Coomassie blue-stained, 12% gel) of individual lysate extracted from *E. coli* cells expressing the 126-kDa CyaA-Hly wild-type (Wt) or its mutant toxins together with the 21-kDa CyaC-acyltransferase protein. Lane M denotes standard protein markers. Lane 1 represents cell lysate containing the pET-17b vector (a negative control). Lanes 2–6 represent lysate supernatants containing the Wt toxin, G530A, G533A, G537A and G544A mutants, respectively. (B) Western blot analysis of A. Lane M is pre-stained standard protein markers.

soluble forms with yields comparable to the wild-type toxin, suggesting that each individual substitution did not have an adverse effect on the overall folding of the mutant molecules. Moreover, all the CyaA-Hly mutants were still recognized by anti-RTX specific antibodies in Western blotting, but not for the 21-kDa protein band, confirming their RTX identity unchanged, albeit with some degradation products detected by such antibodies (Fig. 2B). It is worth noting that the 126-kDa CyaA-Hly protein, like its 100-kDa CyaA-RTX subdomain fragment (Pojanapotha et al., 2011), showed a retarded migration on SDS–PAGE with a size much larger than the 116-kDa β-galactosidase standard marker (*see* Fig. 2B). However, an explanation for its anomalous migration behavior in SDS-gels remains unclear.

3.2. Functional consequences of individual Gly-to-Ala mutations and significant contribution of a GXXGXXXG motif

To determine mutational effects on toxicity of the four CyaA-Hly mutants (G530A, G533A, G537A and G544A), we tested whole cell lysate containing each mutant for their relative hemolytic activity against sheep erythrocytes. As shown in Fig. 3, hemolysis data recorded after 5-h incubation revealed that G530A, G533A and G537A mutants exhibited a substantial decrease in hemolytic activity, giving only 4.7 ± 0.2, 6.5 ± 0.3 and 4.1 ± 0.2% hemolysis, respectively. However, the G544A mutant still retained high hemolytic activity (75.3 ± 1.5%) comparable to the wild-type toxin (73.8 ± 1.1%). Thus, these results suggest that Gly^{530}, Gly^{533} and Gly^{537}, but not Gly^{544}, play an indispensible role in CyaA-Hly hemolysis.

It is noteworthy that these three crucial Gly residues, $Gly^{530}XXGly^{533}XXXGly^{537}$, can be arranged as a GXXGXXXG motif that has been described to promote helix–helix interactions (Bass et al., 2002; Dong et al., 2012), albeit some variations observed among the GXXG/GXXXG patterns, *e.g.* $G^{79}XXXG^{83}XXG^{86}$ of human erythrocyte GpA (glycophorin A) (Russ and Engelman, 2000), $G^{14}XXXG^{18}XXXG^{22}$ found in TM domain of *Helicobacter pylori* VacA (vacuolating toxin) (Kim et al., 2004) and $G^{101}XXG^{104}XXXG^{108}$ in TM3 of *E. coli* MscS (small conductive mechanosensitive channel) (Bass et al., 2002) (*see* Fig. 4A). Additionally, the structural role of Gly residues in the $G^{14}XXXG^{18}$ motif has been signified in the *H. pylori* VacA toxin as being shown to be crucial for membrane-channel formation and cytotoxicity (McClain et al., 2003). Moreover, as can be seen from a plausible 3D model of the CyaA-Hly transmembrane hairpin (α2-loop-α3) shown in Fig. 4B, the three Gly side-chains (Gly^{530}_Gly^{533}_Gly^{537}) are located on the same side at the N-terminal end of α2 but they are oriented away from Glu^{570} which is placed on the hydrophilic face of the pore-lining α3 and is

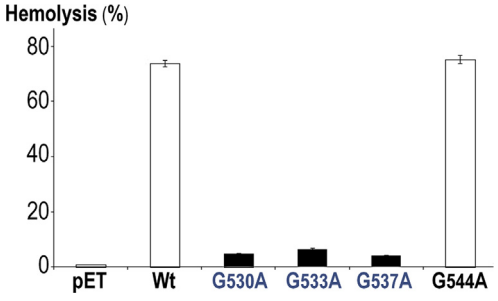

Fig. 3. Hemolytic activity of *E. coli* lysate containing the CyaA-Hly wild-type (Wt) or its mutants (G530A, G533A, G537A and G544A) against sheep erythrocytes. Cell lysate containing the pET-17b vector (pET) was used as a negative control. Error bars represent standard errors of the mean from three independent experiments with each performed in triplicate. Black shaded bars represent the hemolytic activity of the mutants that are significantly different from that of the wild-type (p values ≤ 0.01).

critical for hemolytic activity (Kurehong et al., 2011). Thus, if the CyaA-Hly pore assembly involves the helix–helix association of α2-loop-α3 TM hairpins through the utility of this GXXGXXXG element, the detrimental effects on hemolytic activity observed for the three Gly-to-Ala mutations (G530A, G533A, G537A) could possibly be due to the diminished helix-packing interactions between these critical Gly residues ($Gly^{530}XXGly^{533}XXXGly^{537}$) and their counterpart side-chains in adjacent helices. These mutations would therefore disturb the hemolytic pore assembly in the target erythrocyte membrane (*see* more discussion below).

3.3. Structural model of CyaA-Hly α2–α3 trimeric pore and implications for functional importance of the Gly cluster

Further attempts were made to construct a 3D-modeled structure of the CyaA-Hly pore based on our quantitative hemolysis assays as previously revealing that the CyaA-Hly domain could function cooperatively by forming a trimeric pore with a Hill coefficient of ~3 (Kurehong et al., 2015). Accordingly, we modeled a trimeric assembly of the CyaA-TM hairpin (α2-loop-α3) selected from the best hairpin-packing arrangement using the ZDOCK algorithm that has proven effective for prediction of homo-oligomeric TM helical complexes (Pierce et al., 2014). It appears that the CyaA-Hly pore structure bears a resemblance to the trimeric structure of another α-pore-forming toxin (PFT), the *Bacillus thurienensis* Cry4Ba mosquito-active toxin (Ounjai et al., 2007; Juntadech et al., 2014; Sriwimol et al., 2015), although these two bacterial PFTs have no sequence or structural similarities outside of their pore-lining constituents. Hence, nature has apparently developed a similar design for the two toxin-induced pores, by diverse evolutionary pathways.

As with PFTs which are a large family of proteins produced by bacteria but having also evolved in plants and animals (Szczesny et al., 2011; Xiang et al., 2014), their mechanism of action would generally involve protein–protein and/or protein-membrane interactions, and a particular protein folding pathway underlying conformational transitions from a soluble monomer to a membrane-inserted pore complex (Benke et al., 2015; Sriwimol et al., 2015). Accordingly, such analogous principles have been exploited by bacterial pathogens as well as higher eukaryotes either for attack or for defense (Szczesny et al., 2011; Xiang et al., 2014). Thus, it has been hypothesized that these PFTs have a variety of oligomeric states ranging from small oligomers to large assemblies (*e.g.*, cholesterol dependent cytolysins) (Reboul et al., 2014). Although the lack of pore architectures in a biologically relevant form still confines the information on their oligomeric states, it is possible that many if not all PFTs are required to associate to form functional pores.

As illustrated in Fig. 4C, the CyaA-Hly pore structure is basically stabilized by the inter-helical packing of the Gly cluster (Gly^{530}_Gly^{533}_Gly^{537}) complementarily against Ala^{591}, Ala^{587} and Ala^{583}, respectively, which are located on the C-terminus of α3 in an adjacent hairpin. Notably, a flat helix surface formed by this N-terminal Gly cluster would provide a short inter-helical axial distance between the neighboring hairpins. In this close positioning, the three critical Gly residues which lack side-chains could make possible inter-helical interactions based on a "knobs into holes" arrangement with their small counterparts, *i.e.* Ala^{583}, Ala^{587} and Ala^{591}. Moreover, inter-helical H-bonds between C_α–H atoms of the Gly cluster and carbonyl oxygen atoms of the three-Ala backbone could also possibly promote stable packing of the three TM hairpins (Senes et al., 2001), leading to CyaA-Hly induced pore assembly (*see* Fig. 4C, *inset*). Thus, this trimeric pore model is quite consistent with the mutagenesis results as demonstrated above (*see* Fig. 3). Taken together, to the best of our knowledge, this study is the first

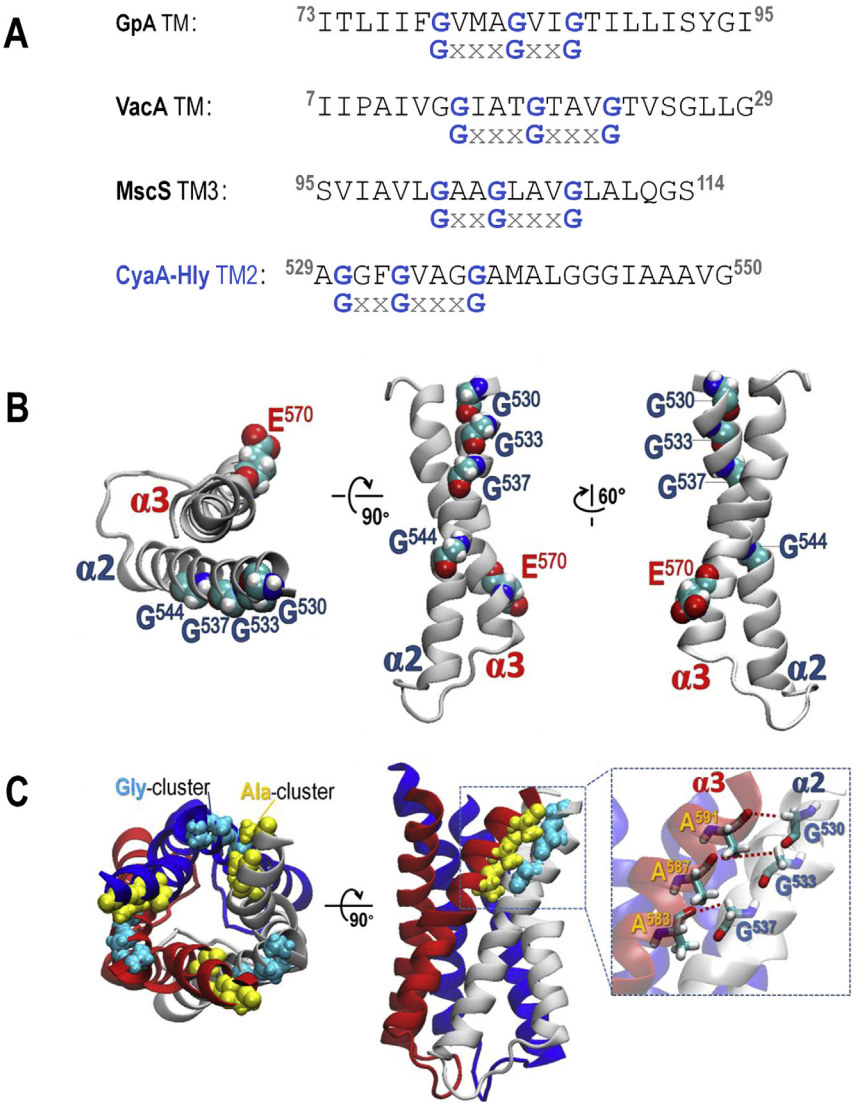

Fig. 4. (A) Representative sequence variations of GXXXG motifs; GpA TM (human erythrocyte glycophorin A transmembrane) containing the GXXXGXXG motif; VacA TM (*H. pylori* VacA toxin transmembrane) containing the GXXXGXXXG motif; MscS TM3 (transmembrane α3 of *E. coli* small conductance mechanosensitive channel) and CyaA TM2 (transmembrane α2 of *B. pertussis* CyaA toxin) containing the same GXXGXXXG motif. (B) Homology-based structure of the α2-loop-α3 TM hairpin of CyaA-Hly. Top (left panel) and side (middle and right panels) views of the TM hairpin. The series of four Gly residues (Gly^{530}, Gly^{533}, Gly^{537} and Gly^{544}) lying on the same face of α2 and one highly conserved negative charge in α3 (Glu^{570}) are depicted as van der Waals (vdW) spheres. (C) Top and side views (left and right panels, respectively) of 3D-modeled structure of CyaA-Hly α2–α3 trimeric pore, showing a flat hydrophobic surface at the N-terminus of α2 created by the Gly^{530}XXGly^{533}XXXGly^{537} cluster (blue vdW spheres) complementarily against the Ala^{583}XX-XAla^{587}XXXAla^{591} cluster (yellow vdW spheres) located at the C-terminus of α3. *Inset*, the zoomed region illustrating plausible inter-helical H-bonds (red dash lines) between C_α–H atoms of the Gly^{530}_Gly^{533}_Gly^{537} cluster and carbonyl oxygen atoms of the Ala^{583}_Ala^{587}_Ala^{591} backbone. (For interpretation of the references to color in this figure legend, the reader is referred to the web version of this article.)

demonstration of a functional importance of the Gly^{530}_-Gly^{533}_Gly^{537} cluster in the CyaA-Hly pore-forming toxin. This three-Gly cluster which is arranged as a GXXGXXXG motif could conceivably drive the association of α2-loop-α3 TM hairpins, leading to toxin trimerization and hemolytic pore formation. Nevertheless, further detailed investigation to find whether this critical Gly cluster (Gly^{530}XXGly^{533}XXXGly^{537}) as well as its plausible interacting counterpart (Ala^{583}XXXAla^{587}XXXAla^{591}) definitely contributes toward the trimerization of the CyaA-Hly toxin is of great interest.

Acknowledgments

This work was supported in part by grants from the Thailand Research Fund (MRG-5480261 to N.T.), Higher Educational Research Promotion, the Commission of Higher Education Commission (CHE), Ministry of Education (SURDI-CHE 57/01/011 to B.P.) and Mahidol University (MU 49/2557). A Ph.D. scholarship from CHE (to S.J.) and a Royal Golden Jubilee Ph.D. scholarship (to C.K.) are gratefully acknowledged.

Transparency document

Transparency document related to this article can be found online at http://dx.doi.org/10.1016/j.toxicon.2015.09.006.

Appendix A. Supplementary data

Supplementary data related to this article can be found at http://dx.doi.org/10.1016/j.toxicon.2015.09.006.

References

Bass, R.B., Strop, P., Barclay, M., Rees, D.C., 2002. Crystal structure of *Escherichia coli* MscS, a voltage-modulated and mechanosensitive channel. Science 298, 1582–1587.

Bellalou, J., Sakamoto, H., Ladant, D., Geoffroy, C., Ullmann, A., 1990. Deletions affecting hemolytic and toxin activities of *Bordetella pertussis* adenylate cyclase. Infect. Immun. 58, 3242–3247.

Benke, S., Roderer, D., Wunderlich, B., Nettels, D., Glockshuber, R., Schuler, B., 2015. The assembly dynamics of the cytolytic pore toxin ClyA. Nat. Commun. 6, 6198.

Chenal, A., Karst, J.C., Sotomayor Perez, A.C., Wozniak, A.K., Baron, B., England, P., Ladant, D., 2010. Calcium-induced folding and stabilization of the intrinsically disordered RTX domain of the CyaA toxin. Biophys. J. 99, 3744–3753.

Cheung, G.Y., Dickinson, P., Sing, G., Craigon, M., Ghazal, P., Parton, R., Coote, J.G., 2008. Transcriptional responses of murine macrophages to the adenylate cyclase toxin of *Bordetella pertussis*. Microb. Pathog. 44, 61–70.

Dong, H., Sharma, M., Zhou, H.X., Cross, T.A., 2012. Glycines: role in α-helical membrane protein structures and a potential indicator of native conformation. Biochemistry 51, 4779–4789.

Guermonprez, P., Khelef, N., Blouin, E., Rieu, P., Ricciardi-Castagnoli, P., Guiso, N., Ladant, D., Leclerc, C., 2001. The adenylate cyclase toxin of *Bordetella pertussis* binds to target cells via the alpha(M)beta(2) integrin (CD11b/CD18). J. Exp. Med. 193, 1035–1044.

Hackett, M., Guo, L., Shabanowitz, J., Hunt, D.F., Hewlett, E.L., 1994. Internal lysine palmitoylation in adenylate cyclase toxin from *Bordetella pertussis*. Science 266, 433–435.

Humphrey, W., Dalke, A., Schulten, K., 1996. VMD: visual molecular dynamics. J. Mol. Graphics 14, 33–38.

Juntadech, T., Kanintronkul, Y., Kanchanawarin, C., Katzenmeier, G., Angsuthanasombat, C., 2014. Importance of polarity of the α4-α5 loop residue-Asn^{166} in the pore-forming domain of the *Bacillus thuringiensis* Cry4Ba toxin: implications for ion permeation and pore opening. Biochim. Biophys. Acta 1838, 319–327.

Karst, J.C., Ntsogo Enguene, V.Y., Cannella, S.E., Subrini, O., Hessel, A., Debard, S., Ladant, D., Chenal, A., 2014. Calcium, acylation, and molecular confinement favor folding of *Bordetella pertussis* adenylate cyclase CyaA toxin into a monomeric and cytotoxic form. J. Biol. Chem. 289, 30702–30716.

Karst, J.C., Sotomayor Perez, A.C., Guijarro, J.I., Raynal, B., Chenal, A., Ladant, D., 2010. Calmodulin-induced conformational and hydrodynamic changes in the catalytic domain of *Bordetella pertussis* adenylate cyclase toxin. Biochemistry 49, 318–328.

Kim, S., Chamberlain, A.K., Bowie, J.U., 2004. Membrane channel structure of *Helicobacter pylori* vacuolating toxin: role of multiple GXXXG motifs in cylindrical channels. Proc. Natl. Acad. Sci. U. S. A. 101, 5988–5991.

Kurehong, C., Kanchanawarin, C., Powthongchin, B., Katzenmeier, G., Angsuthanasombat, C., 2015. Membrane-pore forming characteristics of the *Bordetella pertussis* CyaA-hemolysin domain. Toxins 7, 1486–1496.

Kurehong, C., Powthongchin, B., Thamwiriyasati, N., Angsuthanasombat, C., 2011. Functional significance of the highly conserved Glu^{570} in the putative pore-forming helix 3 of the *Bordetella pertussis* haemolysin toxin. Toxicon 57, 897–903.

Li, E., Wimley, W.C., Hristova, K., 2012. Transmembrane helix dimerization: beyond the search for sequence motifs. Biochim. Biophys. Acta 1818, 183–193.

Linhartova, I., Bumba, L., Masin, J., Basler, M., Osicka, R., Kamanova, J., Prochazkova, K., Adkins, I., Hejnova-Holubova, J., Sadilkova, L., Morova, J., Sebo, P., 2010. RTX proteins: a highly diverse family secreted by a common mechanism. FEMS Microbiol. Rev. 34, 1076–1112.

McClain, M.S., Iwamoto, H., Cao, P., Vinion-Dubiel, A.D., Li, Y., Szabo, G., Shao, Z., Cover, T.L., 2003. Essential role of a GXXXG motif for membrane channel formation by *Helicobacter pylori* vacuolating toxin. J. Biol. Chem. 278, 12101–12108.

Melnyk, R.A., Kim, S., Curran, A.R., Engelman, D.M., Bowie, J.U., Deber, C.M., 2004. The affinity of GXXXG motifs in transmembrane helix-helix interactions is modulated by long-range communication. J. Biol. Chem. 279, 16591–16597.

Melvin, J.A., Scheller, E.V., Miller, J.F., Cotter, P.A., 2014. *Bordetella pertussis* pathogenesis: current and future challenges. Nat. Rev. Microbiol. 12, 274–288.

Mueller, B.K., Subramaniam, S., Senes, A., 2014. A frequent, GxxxG-mediated, transmembrane association motif is optimized for the formation of interhelical Cα-H hydrogen bonds. Proc. Natl. Acad. Sci. U. S. A. 111, 888–895.

Ounjai, P., Unger, V.M., Sigworth, F.J., Angsuthanasombat, C., 2007. Two conformational states of the membrane-associated *Bacillus thuringiensis* Cry4Ba δ-endotoxin complex revealed by electron crystallography: implications for toxin-pore formation. Biochem. Biophys. Res. Commun. 361, 890–895.

Pierce, B.G., Wiehe, K., Hwang, H., Kim, B.H., Vreven, T., Weng, Z., 2014. ZDOCK server: interactive docking prediction of protein-protein complexes and symmetric multimers. Bioinformatics 30, 1771–1773.

Pojanapotha, P., Thamwiriyasati, N., Powthongchin, B., Katzenmeier, G., Angsuthanasombat, C., 2011. *Bordetella pertussis* CyaA-RTX subdomain requires calcium ions for structural stability against proteolytic degradation. Protein Expr. Purif. 75, 127–132.

Powthongchin, B., Angsuthanasombat, C., 2008. High level of soluble expression in *Escherichia coli* and characterisation of the CyaA pore-forming fragment from a *Bordetella pertussis* Thai clinical isolate. Arch. Microbiol. 189, 169–174.

Powthongchin, B., Angsuthanasombat, C., 2009. Effects on haemolytic activity of single proline substitutions in the *Bordetella pertussis* CyaA pore-forming fragment. Arch. Microbiol. 191, 1–9.

Reboul, C.F., Whisstock, J.C., Dunstone, M.A., 2014. A new model for pore formation by cholesterol-dependent cytolysins. PLoS Comput. Biol. 10, e1003791.

Russ, W.P., Engelman, D.M., 2000. The GxxxG motif: a framework for transmembrane helix-helix association. J. Mol. Biol. 296, 911–919.

Sakamoto, H., Bellalou, J., Sebo, P., Ladant, D., 1992. *Bordetella pertussis* adenylate cyclase toxin. Structural and functional independence of the catalytic and hemolytic activities. J. Biol. Chem. 267, 13598–13602.

Senes, A., Engel, D.E., DeGrado, W.F., 2004. Folding of helical membrane proteins: the role of polar, GxxxG-like and proline motifs. Curr. Opin. Struct. Biol. 14, 465–479.

Senes, A., Gerstein, M., Engelman, D.M., 2000. Statistical analysis of amino acid patterns in transmembrane helices: the GxxxG motif occurs frequently and in association with beta-branched residues at neighboring positions. J. Mol. Biol. 296, 921–936.

Senes, A., Ubarretxena-Belandia, I., Engelman, D.M., 2001. The Cα-H···O hydrogen bond: a determinant of stability and specificity in transmembrane helix interactions. Proc. Natl. Acad. Sci. U. S. A. 98, 9056–9061.

Sriwimol, W., Aroonkesorn, A., Sakdee, S., Kanchanawarin, C., Uchihashi, T., Ando, T., Angsuthanasombat, C., 2015. Potential pre-pore trimer formation by the *Bacillus thuringiensis* mosquito-specific toxin: molecular insights into a critical prerequisite of membrane-bound monomers. J. Biol. Chem. 290, 20790–20803.

Szczesny, P., Iacovache, I., Muszewska, A., Ginalski, K., van der Goot, F.G., Grynberg, M., 2011. Extending the aerolysin family: from bacteria to vertebrates. PLoS One 6, e20349.

Van Der Spoel, D., Lindahl, E., Hess, B., Groenhof, G., Mark, A.E., Berendsen, H.J., 2005. GROMACS: fast, flexible, and free. J. Comput. Chem. 26, 1701–1718.

Walther, T.H., Ulrich, A.S., 2014. Transmembrane helix assembly and the role of salt bridges. Curr. Opin. Struct. Biol. 27, 63–68.

Xiang, Y., Yan, C., Guo, X., Zhou, K., Li, S., Gao, Q., Wang, X., Zhao, F., Liu, J., Lee, W.-H., Zhang, Y., 2014. Host-derived, pore-forming toxin-like protein and trefoil factor complex protects the host against microbial infection. Proc. Natl. Acad. Sci. U. S. A. 111, 6702–6707.